이학박사 학위논문

Gremlin-1 Induces BMP-Independent Tumor Cell Proliferation, Migration, and Invasion

그렘린-1에 의한 암세포의 증식, 이동 및 침윤에 관한 연구

2012년 8월

서울대학교 대학원

협동과정 종양생물학 전공

김 민 수

그렘린-1에 의한 암세포의 증식, 이동 및 침윤에 관한 연구

지도교수 정 준 호

이 논문을 이학박사 학위논문으로 제출함.

2012 년 4 월

서울대학교 대학원

협동과정 종양생물학 전공

김 민 수

김민수의 이학박사 학위논문을 인준함.

2012 년 6 월

위 원 장 _____

부위원장 _____

위 원 _____

위 원 _____

위 원 _____

Gremlin-1 Induces BMP-Independent Tumor Cell Proliferation, Migration, and Invasion

by

Minsoo Kim

(Directed by prof. Junho Chung, M.D., Ph.D.)

A Thesis Submitted to the Interdisciplinary Graduate Program in Partial Fulfillment of the Requirement of the Degree of Doctor of Philosophy in Cancer Biology at Seoul National University

June, 2012

Approved by Thesis Committee :

Professor_____Chairperson

Professor_____Vice Chairperson

Professor_____

Professor_____

Professor_____

Abstract

Gremlin-1, a bone morphogenetic protein (BMP) antagonist, is overexpressed in various cancerous tissues but its role in carcinogenesis has not been established. Here, we report that gremlin-1 binds various cancer cell lines and this interaction is inhibited by our newly developed gremlin-1 antibody, GRE1. Gremlin-1 binding to cancer cells was unaffected by the presence of BMP-2, BMP-4, and BMP-7. In addition, the binding was independent of vascular endothelial growth factor receptor-2 (VEGFR2) expression on the cell surface. Addition of gremlin-1 to A549 cells induced a fibroblast-like morphology and decreased E-cadherin expression. In a scratch wound healing assay, A549 cells incubated with gremlin-1 or transfected with gremlin-1 showed increased migration, which was inhibited in the presence of the GRE1 antibody. Gremlin-1 transfected A549 cells also exhibited increased invasiveness as well as an increased growth rate. These effects were also inhibited by the addition of the GRE1 antibody. In conclusion, this study demonstrates that gremlin-1 directly interacts with cancer cells in a BMP- and VEGFR2-independent manner and can induce cell migration, invasion, and proliferation.

Keywords : gremlin-1, cancer cell line, A549, proliferation, Migration, Invasion, Phage display, Monoclonal antibody

Student number : 2006-22170

TABLE OF CONTENTS

ABSTRACT····· i

TABLE OF CONTENTS·····iii

LIST OF TABLES·····iv

LIST OF FIGURES ····· v

ABBREVIATIONS·····vii

INTRODUCTION·····1

PURPOSE OF THE STUDY·····11

MATERIALS AND METHODS·····12

RESULTS·····42

DISCUSSION·····59

REFERENCES·····63

ABSTRACT IN KOREAN·····75

LIST OF TABLES

Table 1. Primers for V_{κ} and V_{λ} of rabbit single-chain libraries with long linker·····21

Table 2. Primers for V_H and overlap extension of rabbit single-chain libraries with long linker·····22

LIST OF FIGURES

Figure 1. Structure feature of gremlin-1 protein·····2

Figure 2. Phage-display cycle·····8

Figure 3. Construction of a human Ab library displayed on phage···9

Figure 4. The amplification of V_{κ}, V_{λ}, and V_H sequences for the construction of scFv libraries (long linker)·····19

Figure 5. The overlap extension PCR to combine the rabbit V_L and V_H fragments for the construction of scFv libraries (long linker)·····24

Figure 6. Titration of serum antibodies·····43

Figure 7. Construction of scFv libraries by overlap PCR·····44

Figure 8. The cross-reactivity of scFv clones in phage ELISA·····45

Figure 9. The specificity of the GRE1 antibody·····46

Figure 10. Gremlin-1 interacts with human cancer cell lines·····49

Figure 11. The interaction of gremlin-1 with cancer cells is independent of VEGFR2 expression·····50

Figure 12. Addition of the neutralizing antibody GRE1 does not interrupt the interaction between gremlin-1 and BMPs·····51

Figure 13. Gremlin-1 induces the scattering and migration of A549 cells *in vitro*·····53

Figure 14. Characterization of gremlin-1-transfected A549cell lines ·····57

ABBREVIATIONS

BCC : basal cell carcinoma

BCP : 1-bromo-3-chloro-propane

BMP : bone morphogenetic protein

BMPR: bone morphogenetic protein receptor

BSA : bovine serum albumin

DEPC : diethyl pyrocarbonate

DTT : dithiothreitol

ECM : extracellular matrix

ELISA : enzyme linked immunosorbent assay

EMT : epithelial-mesenchymal transition

FBS : fetal bovine serum

FGF-4: fibroblast growth factor-4

FITC : fluorescein isothiocyanate

HRP : horseradish peroxidase

HUVEC : human umbilical vein endothelial cell

Ig : immunoglobulin

LB : lurie broth

OD : optical density

PBS : phosphate buffered saline

PCR : polymerase chain reaction

RT-PCR : reverse transcription polymerase chain reaction

SB : super broth

scFv : single chain fragment variable

SDF-1 α : stromal cell-derived factor-1 α

SHH: sonic hedgehog

TBS : tris-buffered saline

TGF- β : transforming growth factor beta

VEGFR : vascular endothelial growth factor receptor

V_H : variable heavy chain

V_L : variable light chain

Introduction

Gremlin-1 is a 20.7-kDa protein consisting of 184 amino acids with a cysteine-rich region, a cysteine knot motif, and a structure shared by members of the TGF-β superfamily. This protein is evolutionarily conserved and the human gremlin gene (*GREM1*) has been mapped to chromosome 15q13-q15 (1, 2). The signaling peptide (1-24) and a predicted glycosylation site (42) have been identified. Post-translational modifications include *N*-glycosylation and phosphorylation (Fig. 1) (3). Gremlin-1 is a secreted protein and three isoforms have been reported (4). Isoform 1 is the most common isoform and isoforms 2 and 3 have deletions of amino acids 39~79 and 10~79, respectively.

Bone morphogenetic proteins (BMPs) are members of the transforming growth factor-β (TGF-β) superfamily of growth factors and were originally identified as osteoinductive cytokines (3). BMPs are now known to control various cell functions in multiple organs. Signaling by BMP ligands involves interaction with two transmembrane serine/threonine kinase receptors termed type I (BMPR-I) and type II (BMPR-II).

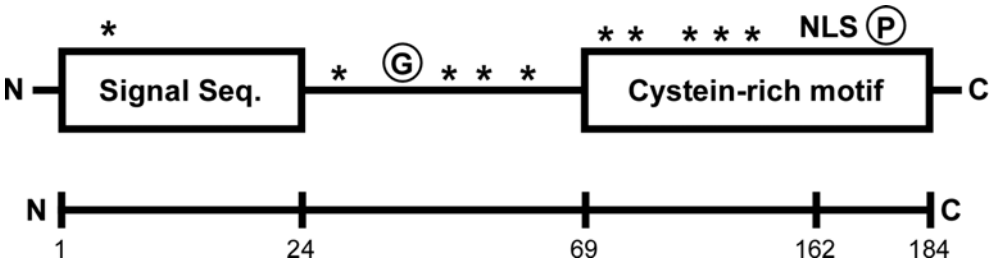

Figure 1. Structure feature of gremlin-1 protein. The predicted positions of structural features of gremlin-1 protein are shown. Signal Seq., signal sequence (position 1-24); Cystein-rich motif (position 69-184); G, glycosylation site (position 42); *, phosphorylation sites (position 6, 29, 44, 47, 55, 66, 76, 77, 88, 102, and 151); P, PKC specific eukaryotic protein phosphorylation site (position 165), NLS, nuclear localization signal sequences (position 145, 166, 163, 164) (3).

Combinations of intracellular and extracellular BMP inhibitors maintain tight control of BMP action in any given tissue. Gremlin-1 forms heterodimers with BMP-2, BMP-4, and BMP-7 and thus inhibits their binding to receptors on the cell surface and subsequent downstream signaling (5-7). In addition, Gremlin-1 plays an important role in regulating BMPs during lung, limb, and kidney development as well as during neural crest cell differentiation (8, 9). Overexpression of gremlin-1 in the distal airway epithelium of transgenic mice caused disruption of normal airway patterning (8, 9). Interestingly, targeted deletion of the gremlin-1 gene also caused loss of normal airway branching and vascular development, lung septation defects, and neonatal lethality in homozygous knockouts (10). In addition to a role in lung development, gremlin-1 expression is crucial for branching morphogenesis and cellular proliferation in other organ systems (11). During vertebrae limb development, gremlin-1 is the major BMP antagonist required for proper limb outgrowth and patterning (12). Gremlin-1 expression is also essential in kidney organogenesis, targeted deletion of gremlin in mice leads to a loss of kidneys due to complete elimination of the metanephric mesenchyme by apoptosis (10). Re-emergence of expression of

this developmental gene in adults results in skeletal and kidney abnormalities. Transgenic mice overexpressing gremlin-1 in bone exhibit decreased bone formation, increased spontaneous fractures, and reduced BMP signaling (13), whereas conditional gremlin-1 deletion in these cells had the opposite phenotype, with enhanced bone-formation and increased responses to BMP stimulation observed (14). Gremlin-1 is part of complex feedback loop, mediating a sonic hedgehog (SHH) signal that regulates fibroblast growth factor-4 (FGF-4) and thus outgrowth and pattering of the limb bud (15, 16). Mice deficient in formin, another component of this signaling loop that induces gremlin-1, have a limb deformity phenotype and reduced gremlin-1 expression (17). Grafting gremlin-1-expressing cells onto the limb buds of these mouse embryos rescues limb development. In the healthy adult kidney, gremlin-1 expression is almost undetectable, whereas it is highly expressed in mesangial cells cultured in high glucose conditions (18) and in patients with diabetic nephropathy (19). Furthermore, elevated gremlin-1 expression has also been found in activated human hepatic stellate cells that trans-differentiate to myofibroblasts in the injured liver, and in mice developing liver fibrosis (20).

In addition to its antagonistic effect on soluble ligands, gremlin-1 interacts intracellularly with the BMP-4 precursor protein and downregulates BMP-4-mediated signaling activity in embryonic lungs (21). A delicate balance exists in tissues between BMP activity and BMP inhibition. Gremlin-1 also interacts with Slit proteins, a family of secreted axonal guidance proteins, and acts as an inhibitor of monocyte chemotaxis (22). Gremlin-1 binding to Slits dependents on its glycosylation and is not interfered with by BMPs. Importantly, gremlin-1 function as inhibitors for monocyte migration induced by stromal cell-derived factor 1α (SDF-1α) or fMLP. The inhibition of SDF-1α-induced monocyte chemotaxis by gremlin-1 is not due to blocking the binding of SDF-1α to its receptor.

Recently it was reported that gremlin-1 binds vascular endothelial growth factor receptor-2 (VEGFR2) in a BMP-independent manner and modulates angiogenesis (23). The expression of gremlin-1 on the levels of mRNA and protein was significantly higher in eutopic endometria of patients with endometriosis than in those from healthy control women (24). The concentration of gremlin-1 in peripheral serum that was collected during the follicular menstrual phase of patients with endometriosis

was significantly higher than that in serum form healthy control women. Gremlin-1 is overexpressed in various human tumors including carcinomas of the cervix, lung, ovary, kidney, breast, colon, and pancreas (25). Furthermore, gremlin-1 expressed by stromal cells in many carcinomas but not in the corresponding normal tissue counterparts (26), but its role in carcinogenesis has not been studied in detail.

Phage display has proven to be a powerful technique for the interrogation of libraries containing millions or even billions of different peptides or proteins (27). One of the most successful applications of phage display has been the isolation of monoclonal antibodies using large phage antibody libraries (28, 29). The phage display system is illustrated Fig. 2. DNA encoding millions of variants of certain ligands (e.g., peptides, proteins, or fragments thereof) is batch-cloned into the phage genome as a fusion to the gene encoding one of the phage coat proteins (pIII, pVI, or pVIII). Upon expression, the coat protein fusion will be incorporated into new phage particles that are assembled in the bacterium. Expression of the fusion product and its subsequent incorporation into the mature phage coat results in the ligand being presented on the phage surface (Fig. 3). Its genetic material resides within the

phage particle. This connection between ligand genotype and phenotype allows the enrichment of specific phage using selection on an immobilized target. Phage that display a relevant ligand will be retained, but nonadherent phage will be washed away. Bound phage can be recovered from the surface, infected into bacteria, replicated to enrich for those clones recovered from the library, and eventually subjected to more detailed analysis. The success of ligand phage display hinges on the synthesis of large combinatorial repertories on phage and the combination of display and enrichment. (27)

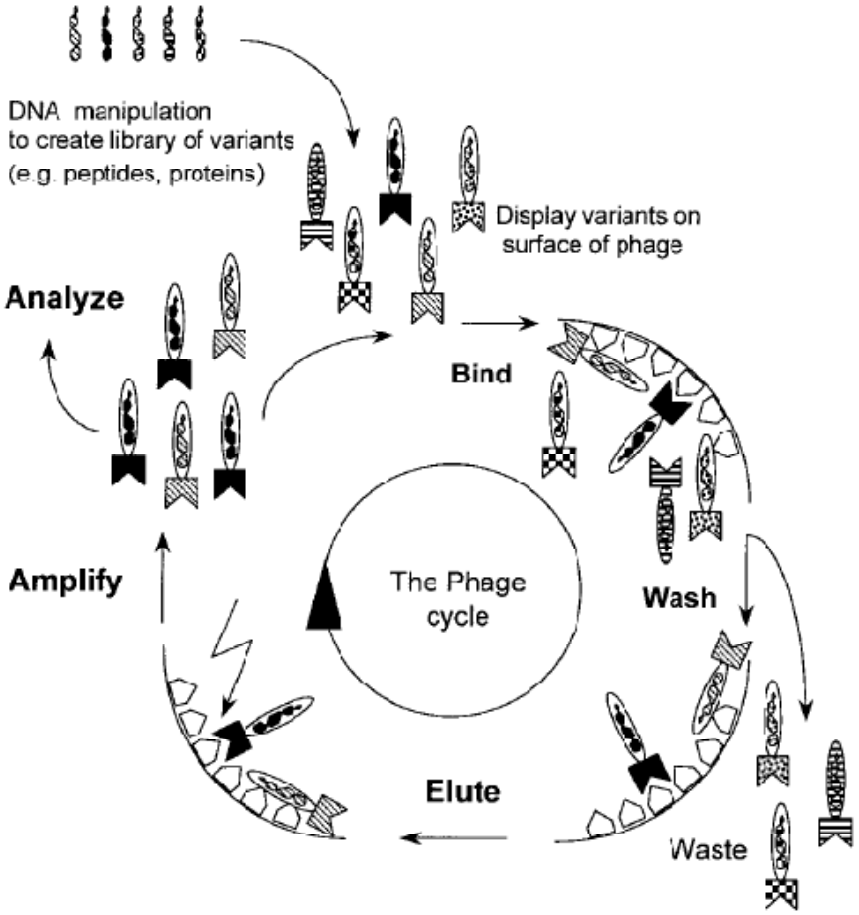

Figure 2. Phage-display cycle. DNA encoding for variants of certain ligand is batch-cloned into the phage genome as part of one of the phage coat proteins (pIII, pVI, or pVIII). Large libraries containing millions of different ligands can be obtained by force-cloning in *E.coli*. From these repertoires, phage carrying specific-binding ligands can be isolated by a series of recursive cycles of selection on Ag, each of which involves bind, washing, elution, and amplification (27).

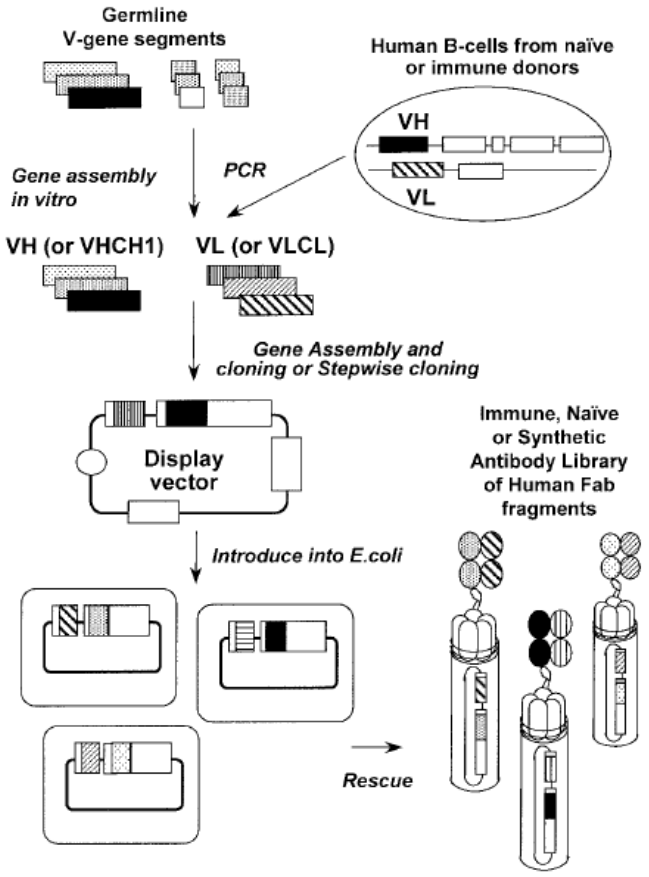

Figure 3. Construction of a human Ab library displayed on phage.

cDNA encoding for the heavy and the light variable regions of Abs (VH, VL) are amplified from human B cells by PCR and assembled. The assembled genes are inserted into a phagemid vector in fram with the gene encoding the CP pIII. The vector is introduced into *E.coli*. After rescue with helper phage, the random combinatorial library of Abs is displayed on phage and selection can be performed (27).

In this study, we report that gremlin-1 directly binds to the cancer cell lines A549, HeLa, A172, and A431. In A549 cells, gremlin-1 induces cell migration, proliferation, and invasion. The interaction with cancer cells was not mediated by VEGFR2, the only known cell surface receptor of gremlin-1, and was unaffected by the presence of BMPs. Gremlin-1-transfected A549 cells showed increased tumor growth *in vivo*, suggesting that gremlin-1 overexpression may play a role in tumorigenesis.

Purpose of the study

Gremlin-1 plays a critical role in regulating BMPs during embryonic development but its expression is down-regulated in normal adult tissues. Gremlin-1 is overexpressed in various human tumors and also in stroma of basal cell carcinoma. However, the function of gremlin-1 in carcinogenesis has not been elucidated yet. This study was aimed to investigate the role of gremlin-1 in cancer by characterization of recombinant gremlin-1 on cancer cells in vitro and characterization of gremlin-1 overexpressing cancer cells in vivo.

Materials and Methods

Cell culture

A549, HeLa, A172, and A431 cells were obtained from the Korean Cell Line Bank (Seoul, Republic of Korea) and human umbilical vein endothelial cells (HUVECs) were obtained from Invitrogen (Carlsbad, CA). A549, A172 and A431 cells were grown in RPMI-1640 media (Welgene, Seoul, Korea) supplemented with 10% FBS (GIBCO, Grand Island, NY). HeLa cells were cultured in MEM media (Welgene) supplemented with 10% FBS. HUVECs were cultured in endothelial cell growth media-2 (EGM-2, Lonza, Walkersville, MD).

Cell transfection

A549 cells (5.0×10^5 cells) were plated 1 day prior to transfection to achieve 70% confluency at the time of transfection. The gremlin cDNA was amplified from a human cervical tissue cDNA library as described previously (25). *Hind*III and *Xho*I restriction sites were introduced at the 5' and 3' ends, respectively,

using the following PCR primers: 5' CCC AAG CTT ATG AGC CGC ACA GCC TAC AC 3' and 5' CCG CTC GAG ATC CAA ATC GAT GGA TAT GC 3'. The PCR product was digested with *Hind*III and *Xho*I and then ligated into the pcDNA3.1/*myc*-His vector (Invitrogen). This expression vector was transfected into cells using the Lipofectamine 2000 reagent (Invitrogen) according to the manufacturer's instructions. To transfect a 100 mm dish of A549 cells, 24 ㎍ of plasmid was mixed with 60 ㎕ of Lipofectamine. Antibiotic selection was performed using 1.0 ㎎/㎖ of G418 (Invitrogen). The selected cells are termed gremlin-1-A549 cells. In a parallel experiment, A549 cells were transfected with pcDNA3.1/*myc*-His vector alone and used as mock-A549 cells.

Expression and purification of gremlin-1

Gene encoding human gremlin-1 and human IgG1-Fc fusion protein was constructed using overlapping PCR as described previously (30). The linker primer sequences (forward and backward for gremlin-1) are as follows; 5' GGC CCC ACC GGC CCC ATC CAA ATC GAT 3', and 5' GGG GCC GGT GGG GCC TCG GGT GGC GGT GGC 3'. The linker primer sequences forward and

backward for human IgG1-Fc are as follows; 5' AAG CTT GTG GCC CAG GCG GCC ATG AGC CGC ACA GCC TAC 3', and 5' GGA TCC TCA TTT TGG CGG GGA CAG GGA GAG 3'. The PCR products were digested with *Hind*III and *BamH*I and cloned into the pCEP4 expression vector (Invitrogen). HEK293F cells (Invitrogen) were cultured in GIBCO FreeStyle^{TM} 293 Expression media (Invitrogen) at a cell density between 0.1 × 10^6 and 2.0 × 10^6 cells/㎖. Cells were grown in disposable Erlenmeyer tissue culture flasks with vented caps (Corning Inc.) at 135 rpm on an orbital shaking incubator (37℃, 8% CO_2, Minitron, INFORS HT, Switzerland). One day prior to transfection, cell cultures were diluted with fresh media to achieve a density of 1.0 × 10^6 cells/ml, which resulted in a density of 2.0 × 10^6 cells/ml on the day of transfection. HEK293F cells were transfected with pCEP4 expression vector using Lipofectamine 2000 (Invitrogen) according to the manufacturer's instructions. Transfected cells were again cultured in the orbital shaking incubator and culture supernatants were harvested the third day after transfection. The gremlin-1-Fc fusion protein was purified using protein A affinity gel chromatography as described previously (30).

Generation of gremlin-1 antibody (GRE1)

Immunization

5 ㎍ of gremlin-1-Fc was mixed in 2 ㎖ of phosphate buffered saline (PBS), incubated at 37℃ for 30 min, emulsified with MPL+TDM+CWS adjuvant (Sigma, St. Louis, Mo) and then injected into New Zealand White rabbits. The immunization was performed three times every three weeks. The antibody titer of immunized rabbits was determined by enzyme linked immunosorbent assay (ELISA) using horseradish peroxidase (HRP)-conjugated mouse anti-rabbit IgG polyclonal antibody (Pierce Chemical Co., Rockford, IL) as secondary antibody.

Isolation of total RNA from rabbit bone marrow and spleen

Total RNA was prepared from the spleen and bone marrow of the rabbits using TRI reagent (Invitrogen). The extracted spleen and bone marrow were homogenized in TRI reagent using a homogenizer at 50% output for 1 min and incubated for 5 min at room temperature. The homogenized samples were centrifuged at 2,500g for 10 min at 4℃. The supernatants were transferred to

50-㎖ centrifuge tubes and 3 ml of 1-bromo-3-chloro-propane (BCP, Sigma) was added to each supernatant. Then they were vortexed for 15 sec and incubated for 15 min at room temperature. The mixtures were centrifuged at 17,500g for 15 min at 4℃ and the upper, colorless aqueous phase was transferred to fresh 50-㎖ centrifuge tubes. Then 15 ㎖ of isopropanol was added and incubated for 10 min at room temperature. After centrifugation at 17,500g for 15 min at 4℃, the supernatant was removed carefully and the pellet was washed with 30 ㎖ of 75% ethanol without resuspension. The pellet was centrifuged again for 10 min. The supernatant was removed and the pellet was air-dried briefly at room temperature. After that, the pellet was dissolved in RNase-free water and stored in -80℃. The RNA concentration was determined by measuring the optical density at 260 nm (40 ng/㎕ RNA gives an OD260 = 1) and the purity was calculated by the ratio of OD260/OD280 (typically in the range of 1.6 to 1.9).

First-strand cDNA synthesis from total RNA

First-strand cDNA was synthesized using SuperScript™ III System for First-Strand cDNA Synthesis kit with oligo(dT) priming

(Invitrogen). For this, 5 ㎍ of the isolated total RNA was mixed with 1 ㎕ of 0.5 ㎍/㎕ oligo(dT), 1 ㎕ of 10 mM dNTP and diethyl pyrocarbonate (DEPC)-treated water to a final volume of 10 ㎕. The mixture was incubated for 5 min at 65℃ and chilled in ice. 2 ㎕ of 10x reaction buffer, 4 ㎕ of 25 mM $MgCl_2$, 2 ㎕ of 100 mM dithiothreitol (DTT), 1 ㎕ of RNase OUT, and 1 ㎕ of Superscript III Reverse Transcriptase were added to the RNA sample and incubated for 50 min at 50℃. After 85℃ incubation for 5 min for reaction termination cooling on ice was done. Then, 1 ㎕ of RNase H was added and incubated for 20 min at 37℃. The first-strand cDNA was stored at -20℃.

First round of PCR

The First-strand cDNAs from spleen and bone marrow of the rabbits were subjected to separate 30 cycles of PCR using Expand High Fidelity PCR System (Roche Molecular Systems, IN, USA). 10 primer combinations for amplification of rabbit V_L (9 x V_κ and 1 x V_λ) coding sequences and 4 combinations for the amplification of rabbit V_H coding sequences (Fig. 4, Table 1) were used together. In each reaction, 1 ㎕ of cDNA was mixed with 60 pmol of each primer, 10

㎕ of 10x reaction buffer, 8 ㎕ of 2.5 mM dNTPs (Promega, Madison, WI), 0.5 ㎕ of Taq DNA polymerase, and water to a final volume of 100 ㎕. The reactions were carried out under the following conditions: 30 cycles of 15 sec at 94℃, 30 sec at 56℃, and 90 sec at 72℃, followed by a final extension for 10 min at 72℃. Fragments with length of approximately 350 base pair (bp) were loaded and run on a 1.5% agarose gel, and purified with QIAEX II Gel Extraction Kit (QIAGEN, Valencia, CA). The purified PCR products were quantified by reading the O.D. at 260 nm (1 O.D. unit = 50 ㎍/㎖).

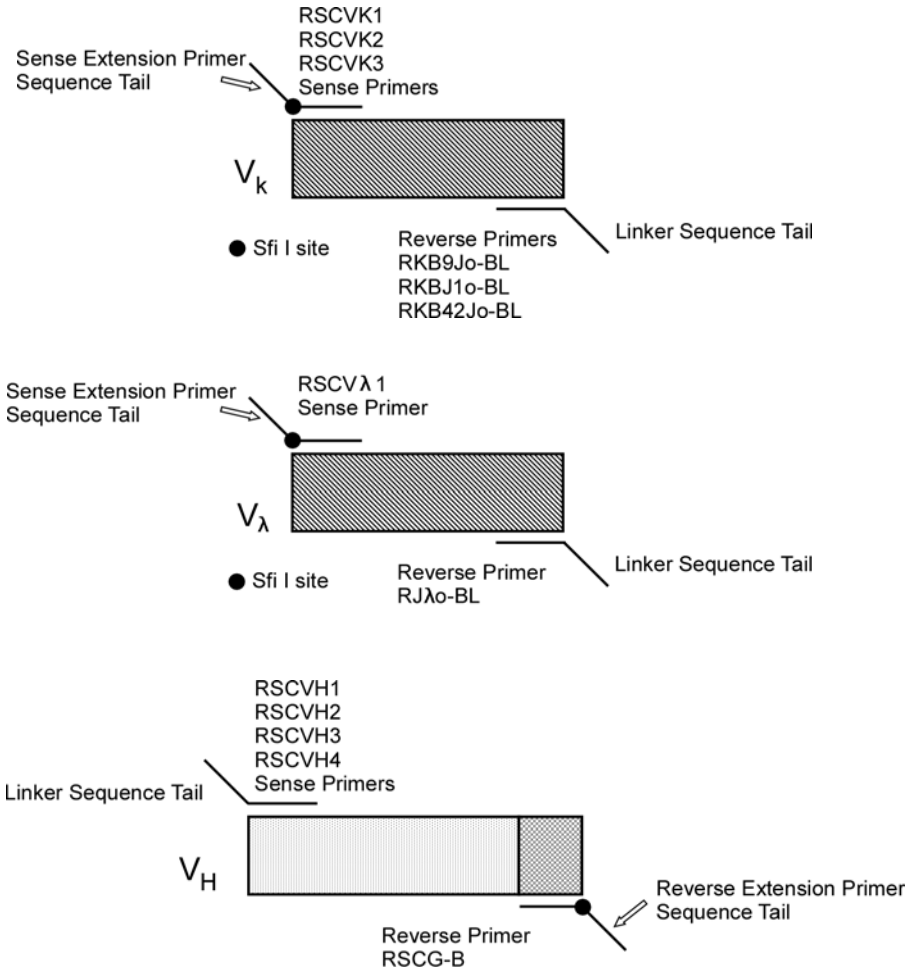

Figure 4. The amplification of V_κ, V_λ, and V_H sequences for the construction of scFv libraries (long linker). Each sense primer is combined with each reverse primer to amplify rabbit V_κ, V_λ, and V_H gene segments from cDNA. The sense primers of V_κ and V_λ have a 5' sequence tail that contains a *Sfi* I site and is recognized by the sense extension primer used in the second-round PCR. The reverse primers of V_κ and V_λ have a linker sequence tail that is used

in the overlap extension. The sense primers of V_H have a sequence tail corresponding to the linker sequence that is used in the overlap extension PCR and the reverse primer of V_H has a sequence tail containing a *Sfi* I site; this tail is recognized by the reverse extension primer used in the second-round PCR.

Table 1. Primers for V_{κ} and V_{λ} of rabbit single-chain libraries with long linker

V_k 5' Sense Primers

RSCVK1
5' GGG CCC AGG CGG CCG ACG TCG TGM TGA CCC AGA CTC CA 3'

RSCVK2
5' GGG CCC AGG CGG CCG AGC TCG ATM TGA CCC AGA CTC CA 3'

RSCVK3
5' GGG CCC AGG CGG CCG AGC TCG TGA TGA CCC AGA CTG AA 3'

V_k 3' Reverse Primers, Long Linker

RKB9J1o-BL
5' GGA AGA TCT AGA GGA ACC ACC CCC ACC ACC GCC CGA GCC ACC GCC ACC AGA GGA TAG GAT CTC CAG CTC GGT CCC 3'

RKB9Jo-BL
5' GGA AGA TCT AGA GGA ACC ACC CCC ACC ACC GCC CGA GCC ACC GCC ACC AGA GGA TAG GAT CTC CAG CTC GGT CCC 3'

RKB42Jo-BL
5' GGA AGA TCT AGA GGA ACC ACC CCC ACC ACC GCC CGA GCC ACC GCC ACC AGA GGA TTT GAC SAC CAC CTC GGT CCC 3'

V_λ 5' Sense Primer

RSCλ 1
5' GGC CCC AGG CGG CCG AGC AGC TCG TGC TGA CTC AGT CCT C 3'

V_λ 3' Reverse Primer, Long Linker

(Linker amino acid sequence: SSGGGGSGGGGGGSSRSS)

RJλo-BL
5' GGA AGA TCT AGA GGA ACC ACC CCC ACC ACC GCC CGA GCC ACC GCC ACC AGA GGA GCC TGT GAC GGT CAG CTG GGT CCC 3'

Table 2. Primers for V_H and overlap extension of rabbit single-chain libraries with long linker

V_H 5' Sense Primers

RSCVH1
5' GGT GGT TCC TCT AGA TCT TCC CAG TCG GTG GAG GAG TCC RGG 3'

RSCVH2
5' GGT GGT TCC TCT AGA TCT TCT CAG TCG GTG AAG GAG TCC GAG 3'

RSCVH3
5' GGT GGT TCC TCT AGA TCT TCC CAG TCG YTG GAG GAG TCC GGG 3'

RSCVH4
5' GGT GGT TCC TCT AGA TCT TCC CAG SAG CAG CTG RTG GAG TCC GG 3'

V_H 3' Reverse Primer

RSCG-B
5' CCT GGC CGG CCT GGC CAC TAG TGA CRG AYG GAG CCT TAG GTT GCC C 3'

Overlap Extension Primers

RSC-F(sense)
5' GAG GAG GAG GAG GAG GAG GCG GGG CCC AGG CGG CCG AGC TC 3'

RSC-B(reverse)
5' GAG GAG GAG GAG GAG GAG CCT GGC CGG CCT GGC CGG CCT GGC CAC TAG TG 3'

Second round of PCR

In the second round of PCR, the first-round V_L products were randomly joined with the first-round V_H products by overlap extension PCR (Fig. 5, Table 2). At least ten reactions for long linker single-chain fragments were performed. In each reaction, 100 ng of purified light-chain product and heavy-chain product were mixed with 60 pmol of each primer, 10 ㎕ of 10x reaction buffer, 8 ㎕ of 2,5 mM dNTPs (Promega), 0.5 ㎕ of Taq DNA polymerase, and water to a final volume of 100 ㎕. The reactions were carried out under the following conditions: 20 cycles of 15 sec at 94℃, 30 sec at 56℃, and 2 min at 72℃, followed by a final extension for 10 min at 72℃. About 700 bp-sized fragments were loaded and run on a 1.5% agarose gel. Then they were purified with QIAEX II Gel Extraction Kit (QIAGEN). The purified PCR products were quantified by reading the O.D. at 260 nm (1 O.D. unit = 50 ㎍/㎖).

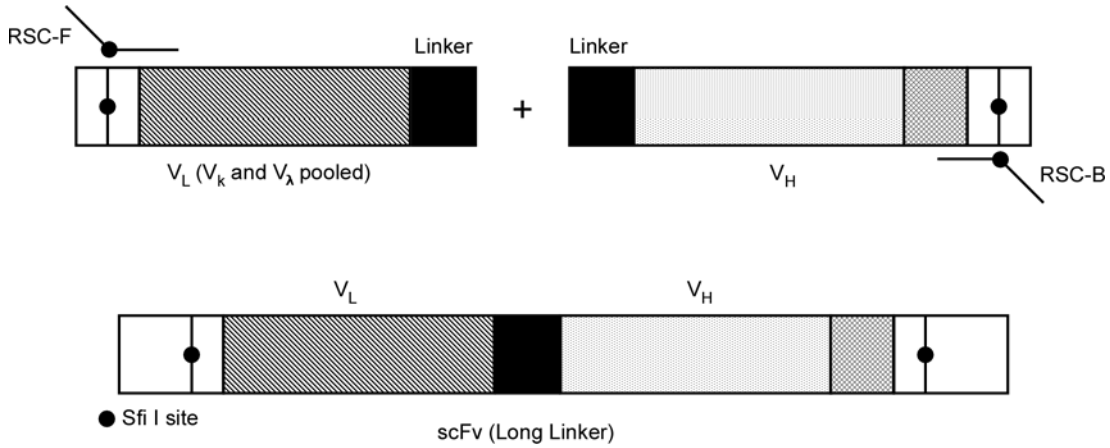

Figure 5. The overlap extension PCR to combine the rabbit V_L and V_H fragments for the construction of scFv libraries (long linker). The sense and reverse extension primers used in this second round of PCR (RSC-F and RSC-B) recognize the sequence tails that were generated in the first round of PCR.

Restriction-digest the purified overlap extension product and the vector DNA

The PCR products and pComb3x vector were digested with *Sfi* I restriction enzyme for cloning. 10 ㎍ of purified overlap PCR products was mixed with 360 units of *Sfi* I (16 units per ㎍ of DNA, Roche Melocular Systems), 20 ㎕ of 10x reaction buffer M, and water to a final volume of 200 ㎕. 20 ㎍ of pComb3x vector was incubated with 120 units of *Sfi* I (6 units per ㎍ of DNA, Roche Melocular Systems), 20 ㎕ of 10x reaction buffer M, and water to a final volume of 200 ㎕. Both digests were incubated for 5 h at 50℃. The digested insert with length about 700 bp was purified on a 1% agarose gel and the vector DNA with length about 3400bp and the stuffer fragment with length about 1600bp were purified on a 0.6% agarose gel as described above.

Ligation of the digested overlap PCR product with the vector DNA

Small-scale ligations were performed to assess the suitability of the vector and inserts for high-efficiency ligation and

transformation. A ligation reaction that contains only the *Sfi* I digestion of the vector DNA was estimated for background ligation which should be less than 5% of library size. For ligation, 140 ng of *Sfi* I-digested and purified vector DNA and 70 ng of *Sfi* I-digested and purified PCR products or stuffer DNA, 4 ㎕ of 5x ligase buffer, 1 ㎕ of T4 DNA ligase (Invitrogen), and water were mixed to a total volume of 20 ㎕. The ligation mixtures were incubated for 4 h at room temperature. 1 ㎕ of the ligation was transformed into 50 ㎕l of ER2738 electrocompetent cells by electroporation with a 0.2 cm cuvette and Gene Pulser (Bio-Rad Laboratories, Hercules, CA) at a condition of 2.5 kV, 25 ㎌, and 200 Ω. The cells were resuspended with 3 ㎖ of SB medium and incubated for 1 h at 37℃ while shaking at 225-250 rpm. The total number of transformants was determined by plating 1 ㎕, 10 ㎕, and 100 ㎕ on LB+carbenicillin plates. Ideally, the final library size should be at least 10^8 colony-forming units (cfu) per ㎍ of vector DNA and should have less than 5% background ligation.

Preparation of electrocompetent *E.coli*

The single *E.coli* colony from a glycerol stock that has been

freshly streaked onto an agar plate was incubated to 15 ㎖ of prewarmed (37℃) SB in a 50 ㎖ polypropylene tube and grew overnight at 250 rpm and 37℃. The next day, 2.5 ㎖ of the culture was diluted into a 2 liter flask with 500 ㎖ of SB, 10 ㎖ of 20% (w/v) glucose, and 5 ㎖ of 1 M $MgCl_2$ and shook at 250 rpm and 37℃ until the OD at 600 nm is about 0.8~0.9. After the proper OD is reached, the flask cultures were poured into a prechilled 500 ㎖ centrifuge bottle and spun at 3000g for 20 min at 4℃. The supernatant was poured off and the pellet was resuspended in 300 ㎖ of prechilled 10% (v/v) glycerol. The resuspended pellet was spun as before. After 3 times of the pellet washing with glycerol, the pellet was resuspended in the remaining volume and stored at −80℃.

Preparation of helper phage

10 ㎕ of ER2738 was inoculated in 10 ml of SB medium and shook at 250 rpm for 1 h at 37℃. A single VCSM13 plaque from a freshly prepared plate was transferred to the culture using a pipet tip. The infected 10 ㎖ culture was transferred to 2 liter Erlenmeyer flask containing 500 ㎖ of prewarmed (37℃) SB

containing kanamycin to a final concentration of 70 ㎍/㎖, and was shaken overnight at 250 rpm and 37℃. The next day, the culture was spun at 2500g for 15 min and the supernatants were incubated in a water bath at 70℃ for 20 min. After spun at 2500g again for 15 min, the supernatants were transferred to fresh 50 ㎖ polypropylene tubes and stored at 4℃.

Library ligation and transformation

Library ligation was carried out using 1.4 ㎍ of *Sfi* I-cut pComb3x, 700 ng of *Sfi* I-cut PCR product, 40 ㎕ of 5x ligase buffer, 10 ㎕ of T4 DNA ligase, and water to a final volume of 200 ㎕. The ligation mixture was incubated overnight at room temperature, followed by ethanol precipitation overnight at -80℃. After spun at full speed in a microcentrifuge for 15 min at 4℃, the supernatant was discarded and the pellet was rinsed twice with 1 ㎖ of 70% (v/v) ethanol and dried briefly. The pellet was dissolved in 15 ㎕ of water. Ligated library sample was transformed into 300 ㎕ of electrocompetent *E.coli* and incubated in 5 ㎖ SB medium for 1 h at 37℃. 10 ㎖ of prewarmed SB medium and 3 ㎕ of 100 ㎎/㎖ carbenicillin were added to the culture. The library size was

determined by plating 0.1 ㎕, 1 ㎕ and 10 ㎕ of the culture on LB plate containing 50 ㎍/㎖ of carbenicillin. The culture was shook for 1 h at 250 rpm and 37℃. 4.5 ㎕ of 100 ㎎/㎖ carbenicillin was added to the culture and shook for an additional hour. The culture was added with 2 ㎖ of VCSM13 helper phage, 183 ㎖ of prewarmed SB and 92.5 ㎕ of 100 ㎎/㎖ carbenicillin and shook for 2 h at 300 rpm and 37℃. 280 ㎕ of 50 ㎎/㎖ Kanamycin was added to the culture and the culture was shaking overnight at 300 rpm and 37℃. The next day, the culture was centrifuged at 3000g for 15 min at 4℃. The bacterial pellet was saved for phagemid DNA preparations and the supernatant was transferred to clean 500 ㎖ centrifuge bottle. After that, 8 g of polyethylene glycol-8000(PEG-8000) and 6 g of NaCl were added. After stored on ice for 30 min, the supernatant was spun at 15000g for 15 min and 4℃. The supernatant was discarded and the phage pellet was resuspended in tris-buffered saline (TBS) containing 1% BSA.

Library panning on an immobilized antigen

Bio-panning was performed by using paramagnetic beads (Dynal Biotech, Lake Success, NY). 3 ㎍ of gremlin-1 was conjugated

with 1 x 10^7 beads at room temperature for 20 h. The beads were washed four times with PBS and incubated with blocking buffer for 1 h at room temperature. The beads conjugated with gremlin-1 were incubated with phages displaying scFvs for 2 h at room temperature. The washing steps were increased from 3 times in the first round to 10 times in fourth round afterward. Bound phages were eluted using 50 ㎕ of 0.1 M glycin/HCl (pH2.2) and were neutralized by 3 ㎕ of 2 M Tris-Cl (pH9.1). This phage-containing supernatant was used to infect ER2738 and the phagemid was rescued with helper phage VCSM13 for overnight amplification. Next day, phage was prepared by adding PEG-8000 and NaCl as described above. Also, the input and output phage titers were determined by plating the phage infected cultures on LB plate containing 50 ㎍/㎖ of carbenicillin.

Selection of clones by phage ELISA

To identify binding scFv from the individual clones selected for further analysis, an ELISA using phage displayed scFv was performed against purified, recombinant gremlin-1. Microtiter plates coated with gremlin-1 were blocked for 1 h at 37℃ using 3%

BSA in PBS. Then phage supernatants were equally mixed with 6% BSA in PBS and incubated for 1 hours at 37℃. After washing with 0.05% PBST, plates were incubated with an HRP-conjugated anti-M13 antibody (1:5,000 dilution; Pierce Chemical Co.). 2, 2'-azino-bis(3-ethylbenzothiazoline-6-sulphonic acid (ABTS) substrate solution (Amresco, Solon, OH) was used for the coloring reaction.

The scFv fragments were converted to full length IgG and overexpressed as described previously [16]. The specificity of the GRE1 antibody was determined using western blot analyses. To determine the specificity of the gremlin-1 antibody GRE1, the culture supernatant of HEK293F cells transfected with pcDNA3.1/*myc*-His-gremlin-1 was resolved by SDS-PAGE as described previously [14]. The blots were incubated with 100 ng/㎖ GRE1 overnight at 4°C, followed by incubation for 1 h at room temperature with HRP-conjugated anti-human IgG (Fc specific, 1:1000 dilution; Pierce Chemical Co.). The blot was visualized using an enhanced chemiluminescence system (Pierce) per the manufacturer's instructions. The gel was visualized using a Coomassie brilliant blue G-250 (Sigma) per the manufacturer's instructions.

RNA isolation and RT-PCR

Total RNA was isolated from A549, HeLa, and HUVEC cells using the TRIzol reagent (Invitrogen) according to the manufacturer's instructions. cDNA was synthesized using the Superscript® III First-Strand Synthesis system (Invitrogen). The primer sequences were as follows: VEGFR-2 forward: 5'-TGATCGGAAATGACACTGGA-3', VEGFR-2 reverse: 5'-TGCTTCACAGAAGACCATGC-3', gremlin-1 forward: 5'-AACAGTCGCACCATCATCAA-3', gremlin-1 reverse: 5'-AATTTCTTGGGCTTGCAGAA-3', GAPDH forward: 5'-AGGTGAAGGTCGGAGTCAACG-3', GAPDH reverse: 5'-AGGGGTCATTGATGGCAACA-3'. The PCR mixtures were prepared according to the manufacturer's instructions with PCR conditions of 35 cycles of 30 sec at 94℃, 30 sec at 56℃, and 1 min at 72℃ on a 2720 Thermal Cycler (Applied Biosystems, Foster City, CA).

Flow cytometry

Adherent cells were trypsinized and washed with 1% (w/v) BSA

in phosphate-buffered saline (PBS). Suspension cells were collected by centrifugation at 500*g* for 2 min and washed with 1% (w/v) BSA in PBS. All cells were incubated with His-tagged gremlin-1 at a final concentration of 100 nM in 1% (w/v) BSA in PBS for 1 h at 37℃. The cells were then washed twice with 1% (w/v) BSA in PBS and incubated for 30 min at 37℃ in the dark with a FITC-conjugated His antibody (Abcam, Cambridge, UK) at a final concentration of 5 ㎍/㎖. Cells were then washed twice with 1% (w/v) BSA in PBS and resuspended in 500 ㎕ of PBS prior to analysis on a FACSCanto II flow cytometer (BD Biosciences, San Jose, CA).

To determine the neutralizing efficacy of the gremlin-1 antibody GRE1, cells were incubated with 100 nM of gremlin-1 and 10 ㎛M of GRE1 in 1% (w/v) BSA in PBS for 1 h at 37℃ and probed with a FITC-conjugated His antibody (Abcam).

A549 cells were treated with 1 ㎛M of BMP-2, BMP-4, or BMP-7 (R&D Systems, Minneapolis, MN) and 100 nM of gremlin-1 simultaneously and incubated for 1 h at 37℃. Cells were probed with FITC-conjugated IgG-Fc specific antibody (5 ㎍/㎖, Invitrogen). Cells were then analyzed on a FACSCanto II flow cytometer.

Western blot analyses

HUVECs, A549 cells, and HeLa cells were lysed in ice-cold lysis buffer [50 mM Tris-HCl (pH 7.4), 150 mM NaCl, 2 mM EDTA, 1% Triton-X 100, 0.1% SDS, 1 mM PMSF] containing a protease inhibitor cocktail (Sigma-Aldrich, St. Louis, MO). Western blots were performed as described previously (31). E-cadherin (1:1,000 dilution; Abcam), VEGFR-2 (1:1,000 dilution; Cell Signaling Technology, Danvers, MA), and β-actin (1:10,000 dilution; Applied Biological Materials, Richmond, BC) antibodies were used as the primary antibodies. The secondary antibodies were horseradish peroxidase (HRP)-conjugated anti-mouse IgG (1:1,000 dilution; Pierce Chemical Co., Rockford, IL) or HRP-conjugated anti-rabbit IgG (1:1,000 dilution; Pierce Chemical Co.). Blots were visualized using an enhanced chemiluminescence system (Pierce) per the manufacturer's instructions.

To analyze E-cadherin expression, A549 cells (1.0×10^5 cells/well) were seeded onto a 60-mm dish and grown to 50% confluence. Cells were treated with 100 nM of His-tagged gremlin-1 for 3 days. Cells were lysed and analyzed by western

blot as described above.

To determine the neutralizing efficacy of the gremlin-1 antibody GRE1, gremlin-1-A549 cells and mock-A549 cells (1.0×10^5 cells/well) were seeded onto a 60-mm dish to 50% confluence. Mock-A549 cells were cultured without treatment and Gremlin-1-A549 cells were cultured for 24 h in the presence of 10 μM GRE1 or control antibody (Palivizumab, Synagis, Abbott Laboratories, Abbott Park, IL). Cells were lysed and analyzed by western blot as described above.

To analyze gremlin-1 expression, the culture supernatants from mock-A549 and gremlin-1-A549 cells were resolved by SDS-PAGE as described above. The blots were incubated for 1 h at room temperature with HRP-conjugated -His antibody (1:1000 dilution, R&D Systems). Blots were visualized using an enhanced chemiluminescence system (Pierce) per the manufacturer's instructions.

Enzyme immunoassay

Microtiter plates (Corning Costar Corp., Cambridge, MA) were

coated with 100 nM of BMP-2, BMP-4, or BMP-7 (R&D Systems) and blocked with 1% (w/v) skim milk in PBS. Gremlin-1 (10 nM) or gremlin-1 (10 nM) plus 500 nM of GRE1 antibody were added to the wells. After washing, plates were incubated with an HRP-conjugated IgG-Fc specific antibody (1:5,000 dilution; Pierce Chemical Co.). 2,2'-azino-bis(3-ethylbenzothiazoline-6-sulphonic acid (ABTS) substrate solution (Amresco, Solon, OH) was used for the coloring reaction as described previously (32). Experiments were performed in triplicate.

Crystal violet staining assay

A549 cells were seeded in 24-well plates (1.0×10^4 cells/well) and treated with 100 nM of gremlin-1 for 3 days. Media was removed and cells were washed with PBS and fixed with 4% paraformaldehyde in PBS for 10 min. Cells were stained with 0.05% crystal violet in distilled water for 30 min. The staining solution was removed and the cells were washed 3 times with PBS as described (33). Images were obtained using a Leica DFL290 camera (Leica Microsystems, Wetzlar, Germany) and analyzed using Leica application suite software (Leica Microsystems)

Immunofluorescence staining

A549 cells (1.5 × 10^4 cells/well) were seeded on glass coverslips coated with poly-L-lysine (100 ㎍/㎖, Sigma) and grown to 50% confluence. Cells were treated with 100 nM of gremlin-1 for 3 days, rinsed in PBS, and fixed in 4% paraformaldehyde in PBS for 30 min at room temperature. Fixed cells were permeabilized with 0.2% Triton X-100 in PBS (PBST) at room temperature for 10 min and then blocked with 1% gelatin in PBST for 30 min at room temperature. Immunofluorescent staining was performed using an E-cadherin antibody (Abcam) followed by an Alexa 488-conjugated secondary antibody (Invitrogen). Nuclei were stained with DAPI (1:1,000 dilution; Invitrogen) and actin filaments were stained using rhodamine-phalloidin (1:1,000 dilution; Invitrogen). Coverslips were mounted on glass slides using aqueous mounting medium with anti-fading agents (Biomeda Corp., Foster City, CA). Images were acquired using a LSM 5 PASCAL Laser Scanning Microscope (Carl Zeiss, Germany) and analyzed using LSM 5 PASCAL software.

Cell migration assay

Cells were seeded in 24-well plates at a density of 1.0×10^5 cells per well. A scratch wound was generated by scratching with a pipette tip. After rinsing with media to remove detached cells, 100 nM of gremlin-1 was added to the cultures for 24 h. Photographic images were taken from each well immediately and again after 24 h using a Leica DFL290 camera (Leica Microsystems). Images were analyzed using Leica application suite software (Leica Microsystems). The distance that cells migrated through the area created by scratching was determined by measuring the wound width at 24 h and subtracting it from the wound width at the start. The values obtained were then expressed as % migration, setting the migrating distance of cells untreated as 100% as described (34).

To determine the neutralizing efficacy of the gremlin-1 antibody GRE1, scratched cells were incubated for 24 h with gremlin-1 alone or plus 10 μM GRE1 (or 10 μM control antibody). The distance was determined as described above.

Using the same protocol, mock transfected A549 cells and gremlin-1 transfected A549 cells were seeded and scratched. Mock-A549 cells were cultured without any treatment while

Gremlin-1-A549 cells were cultured for 24 h in the presence of 10 μM GRE1 or control antibody. The distance was determined as described above. The results were representative of three independent experiments.

Cell invasion assay

Cell invasion assays were performed using ECM coated inner chambers (Chemicon, Temecula, CA) per the manufacturer's instructions. Mock-A549 cells and gremlin-1-A549 cells (3.0×10^5 cells per well) were suspended in 300 $\mu\ell$ of serum-free media. Complete media (500 $\mu\ell$) containing 10% FBS was added to the bottom wells of the plate. Cells were incubated for 48 h. Non-migrating cells were wiped away and washed with PBS. The membranes were fixed with 4% paraformaldehyde in PBS and stained with a crystal violet stain solution (Chemicon). Images were acquired using a Leica DFL290 camera (Leica Microsystems) and analyzed using Leica application suite software. Migrated cells were counted in four separated fields per well. The values obtained were then expressed as % invasion, setting the cell counts of mock-A549 cells as 100%. The results were representative of three

independent experiments.

Cell proliferation assay

Cell proliferation was determined using CellTiter 96 Aqueous One Solution Cell Proliferation Assay (Promega, Madison, WI) following the manufacturer's protocol. Experiments were performed in 96-well plates in RPMI-1640 media supplemented with 10% FBS. Mock-A549 cells and gremlin-1-A549 cells were seeded at a density of 1,000 cells per well. After 24 h, cells were washed twice with serum-free media and cultured in 100 ㎕ of complete media with or without 3 ㎛M of GRE1 antibody. Cell proliferation was determined by using Labsystems Multiskan Ascent Photometric plate reader (Thermo Labsystems, Franklin, MA) for a 96 well plate with a 492 nm filter. Experiments were performed in triplicate.

In vivo tumorigenesis

All animal experiments were authorized by the Institute of Laboratory Animal Resources Seoul National University and Use

Committee (Permit number: SNU-11-0207). Gremlin-1-A549 cells and mock-A549 cells (1.0×10^6 cells/mouse) were injected subcutaneously in the right flank of 4- to 6 week-old female, athymic nude mice (7 mice in each treatment group). Tumor formation and size were assessed weekly by caliper measurements of the length and width of the tumors. Tumor volumes were calculated using the following formula: (Length × Width × Height) / 2 (35).

Results

Generation of anti-gremlin-1 antibody

After immunization with gremlin-1, it was important to determine the titer of antibody in serum with regular intervals during the course of injections. Titration of serum antibody was measured by enzyme immunoassay (Fig. 6). The titer reached an appropriate level after three injections. Total RNA was extracted from rabbit bone marrow and spleen, and RNA quality is assessed by electrophoresis with agarose gel (Figure 7A). Rabbit immune scFv library was constructed using overlap PCR (Figure 7B & 7C). Using phage display, scFv clones were selected from library. These clones showed the cross-reactivity to both human and mouse gremlin-1 in phage ELISA (Fig. 8). The specificity of the GRE1 antibody was determined using western blot analyses (Fig. 9).

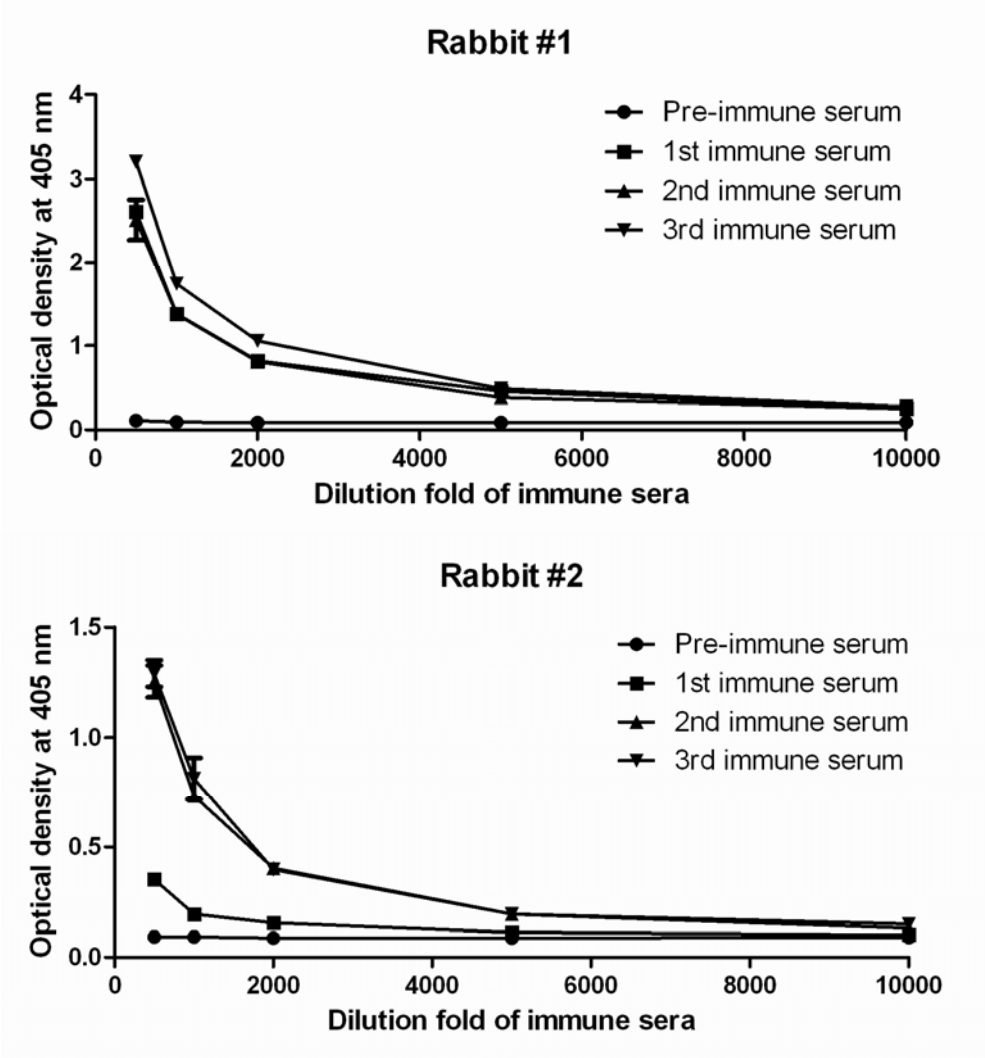

Figure 6. Titration of serum antibodies. The immune titers of antibodies against gremlin-1 in serum were measured by enzyme immunoassay.

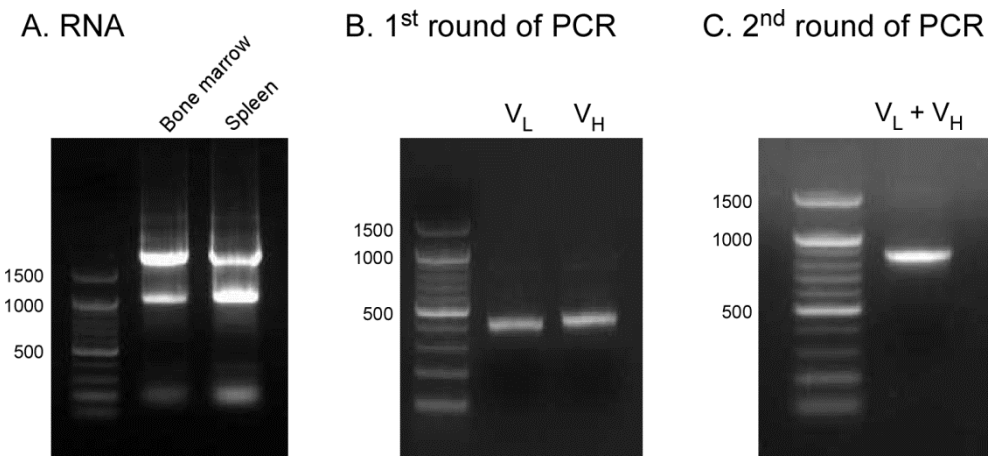

Figure 7. Construction of scFv libraries by overlap PCR. (A) Preparation of mRNA from rabbit bone marrow and spleen. Purified first round PCR fragments of V_L and V_H (B) and overlap PCR fragments (C) were loaded and run on an agarose gel.

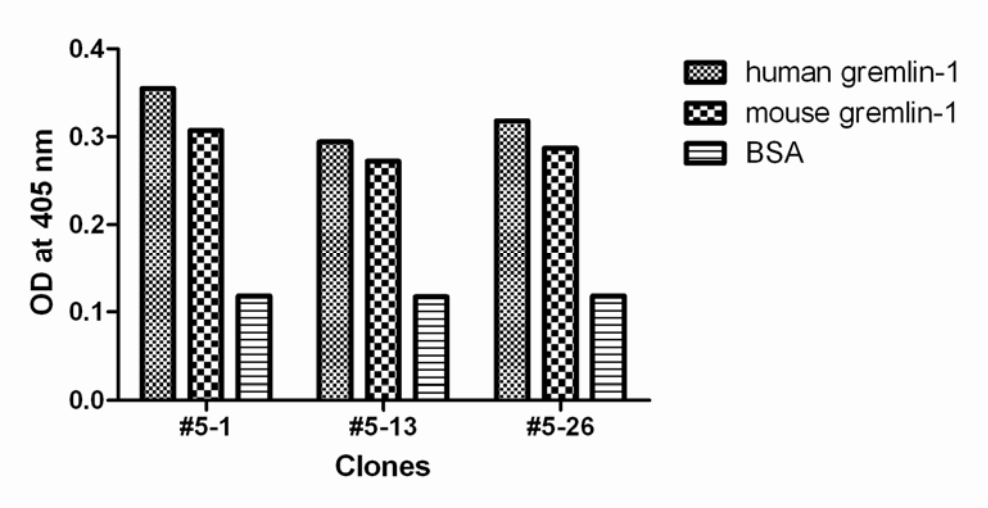

Figure 8. The cross-reactivity of scFv clones in phage ELISA. Gremlin-1 specific binding clones reacted with both human and mouse gremlin-1.

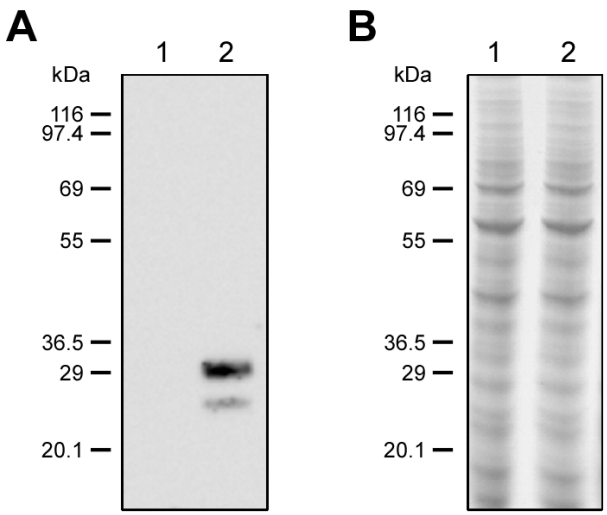

Figure 9. The specificity of the GRE1 antibody. Western blot analysis (A) and Coomassie staining (B) of the culture supernatant of HEK293F transfected with gremlin-1 indicates that GRE1 reacts specifically with gremlin-1. Lanes 1 and 2 were loaded with culture supernatant of HEK293F cells that were mock-transfected or transfected with gremlin-1, respectively. The gremlin-1 protein has post-translational modification sites and exists in two major forms (glycosylated and unglycosylated)(4).

Gremlin-1 directly interacts with human cancer cell lines

The interaction of gremlin-1 with cancer cell lines was analyzed by flow cytometry. Four cancer cell lines, including A549 cells, interacted with gremlin-1 (Fig. 10). The gremlin-1 antibody GRE1 inhibited the binding of gremlin-1 to all cell lines, including A549 (Fig. 10). These data indicate that gremlin-1 directly interacts with cancer cells depending on a motif either co-localized with the epitope of antibody GRE1 or affected by the binding of GRE1. Next, we evaluated whether the interaction of gremlin-1 with the cell lines was mediated by VEGFR2, the only known cell surface receptor of gremlin-1 (23). In HUVECs, the binding of gremlin-1 was not significant (Fig. 11A) but VEGFR2 mRNA and protein expression was confirmed using RT-PCR and immunoblot analyses (Fig. 11B and 11C). However, although gremlin-1 interacted with A549 and HeLa cells (Fig. 10), VEGFR2 mRNA and protein were not detected in these cells as measured by RT-PCR and immunoblot analyses (Fig. 11B and 11C). Therefore, we conclude that gremlin-1 can interact with cancer cells directly and this interaction does not have to be mediated by VEGFR2.

The most characterized function of gremlin-1 is as a BMP antagonist. Therefore, we investigated the influence of BMPs on the interaction of gremlin-1 with A549 cells. Gremlin-1 forms heterodimers with BMP-2, BMP-4, and BMP-7 and interrupts the binding of BMPs to their receptors. In an enzyme immunoassay, gremlin-1 interacted with BMP-2 and BMP-4. Gremlin-1 did not interact with BMP-7 in our experimental conditions and the reason for this is unclear. Addition of the neutralizing antibody GRE1 did not inhibit the interaction of gremlin-1 with BMP-2 or BMP-4 (Fig 12A, $*P<0.05$). In flow cytometric assays, the presence of a molar excess of BMPs did not affect the interaction of gremlin-1 with A549 cells (Fig. 12B). These results indicate that there are likely two separate motifs in gremlin-1 that mediate its interaction with A549 cells and BMPs, and these motifs do not co-localize.

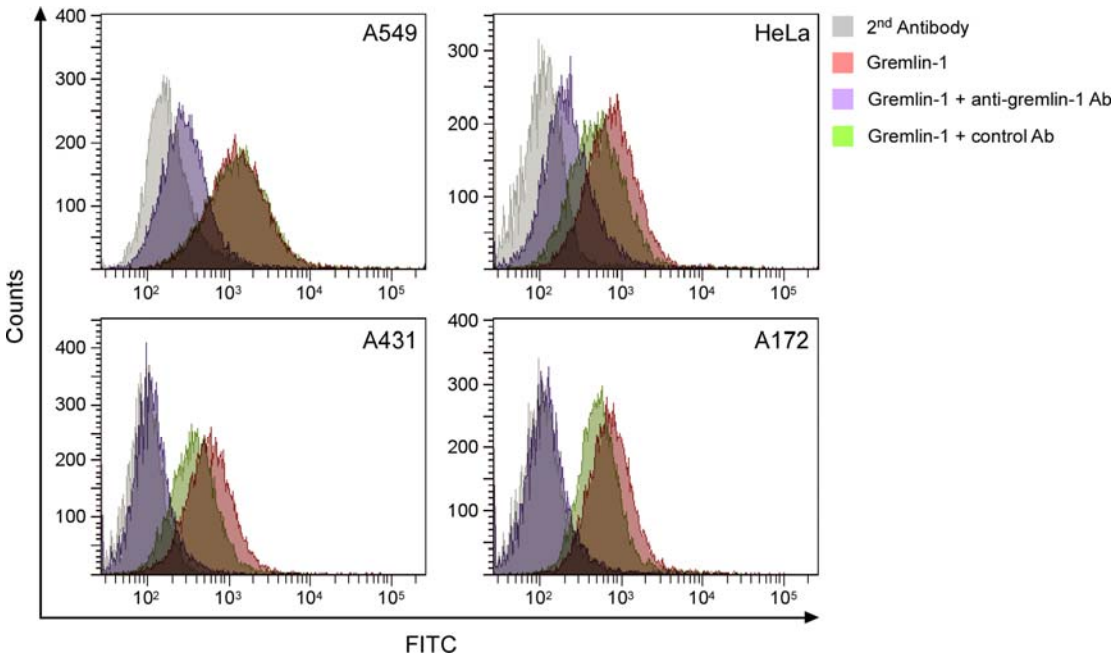

Figure 10. Gremlin-1 interacts with human cancer cell lines. Cells were incubated with gremlin-1, in the presence or absence of the neutralizing antibody GRE1 as described. The four cancer cell lines interacted directly with gremlin-1 and this interaction was inhibited upon the addition of the neutralizing antibody GRE1.

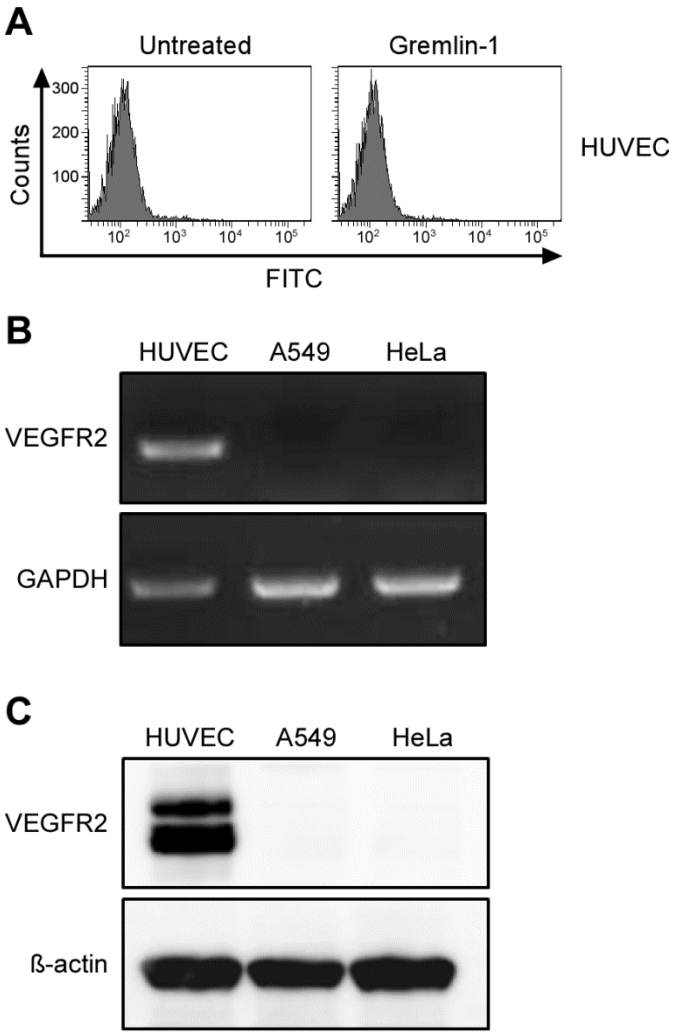

Figure 11. The interaction of gremlin-1 with cancer cells is independent of VEGFR2 expression. (A) Gremlin-1 does not interact with HUVECs as measured by flow cytometry. (B) RT-PCR analysis of VEGFR2 mRNA indicates the presence of VEGFR2 in HUVECs but not in A549 or HeLa cells. (C) Immunoblot analysis using a VEGFR2 antibody indicates that A549 and HeLa cells do not express VEGFR2.

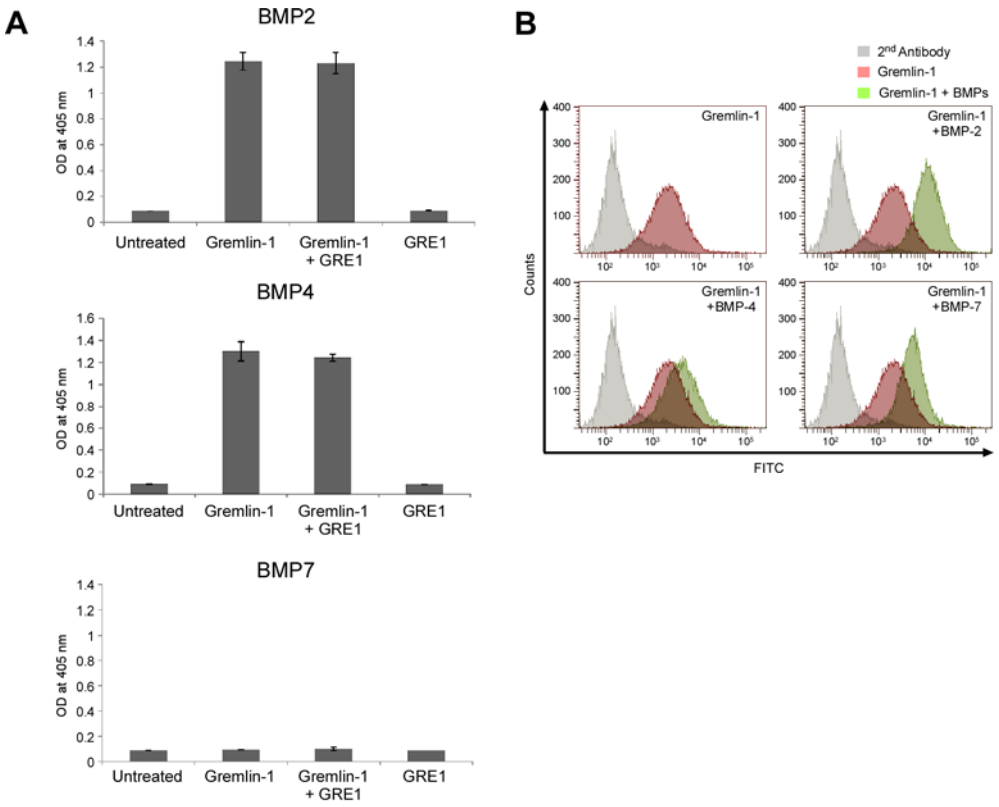

Figure 12. Addition of the neutralizing antibody GRE1 does not interrupt the interaction between gremlin-1 and BMPs. (A) Interaction of gremlin-1 with BMP-2, BMP-4, and BMP-7 as measured by enzyme immunoassay. The neutralizing antibody GRE1 does not affect the interaction between gremlin-1 and BMPs. *P<0.05, Student's *t* test. (B) The interaction of gremlin-1 with A549 cells is unaffected by treatment with a 10 times molar excess of BMP-2, BMP-4, and BMP-7 as measured by flow cytometry.

Gremlin-1 induces A549 cell scattering and migration independent of BMPs

When A549 cells were treated with gremlin-1 for 3 days, the cell morphology became fibroblast-like and the cells became scattered (Fig. 13A). E-cadherin expression was markedly reduced in A549 cells cultured with gremlin-1 as evaluated by immunoblot analysis and immunofluorescence staining (Fig. 13B and 13C). In a scratch wound healing assay, treatment with gremlin-1 for 24 h significantly increased the migration of A549 cells (Fig. 13D, ***P<0.001). This effect was completely abolished upon addition of the neutralizing antibody GRE1 (Fig. 13D, **P<0.01).

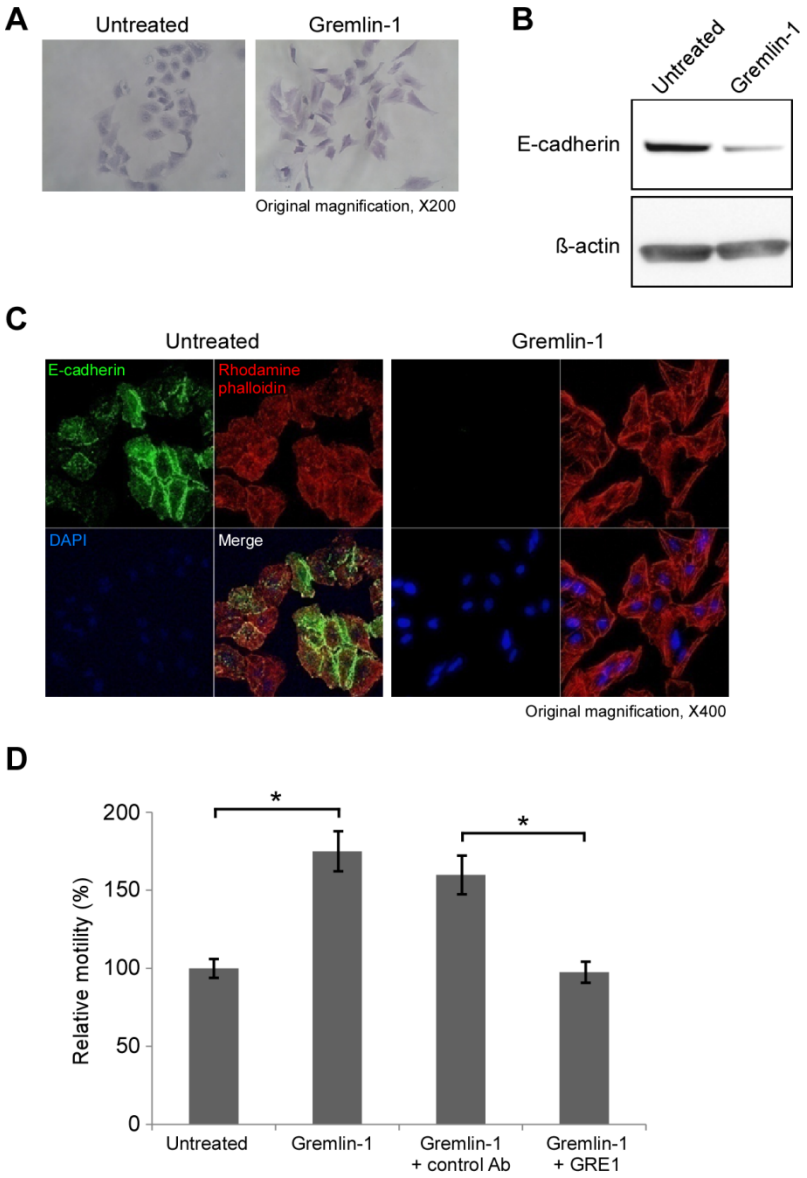

Figure 13. Gremlin-1 induces the scattering and migration of A549 cells *in vitro.* (A) A549 cells appear fibroblast-like after incubation with gremlin-1 for 3 days. (B) E-cadherin protein expression is reduced in A549 cells after incubation with gremlin-1 for 3 days. (C) E-cadherin immunofluorescence (green) in A549 cells is

reduced after incubation with gremlin-1 for 3 days. Nuclei were counterstained with DAPI (blue) and actin filaments were counterstained with rhodamine-phalloidin (red). (D) Migration of A549 cells after incubation with gremlin-1 only or gremlin-1 plus GRE1. Addition of the neutralizing antibody GRE1 abolishes gremlin-1 induced migration. **P<0.01, ***P<0.001, Student's *t* test.

Characterization of gremlin-1 transfected A549 cell lines

Next, we generated stably transfected A549 cell lines containing gremlin-1 (gremlin-1-A549) or empty vector (mock-A549). Using RT-PCR and western blot analyses, we confirmed increased levels of gremlin-1 transcript and protein in the gremlin-1-A549 cells (Fig. 14A). E-cadherin expression was reduced in gremlin-1-A549 cells as compared with mock-A549 cells. However, its expression slightly increased upon addition of the neutralizing antibody GRE1 to the culture media (Fig. 14B). For cell invasion assays, gremlin-1-A549 cells or mock-A549 cells were plated on the upper surface of ECM coated membrane of inner chambers. After 48 h, the cells that migrated through ECM and attached to the bottom of the membrane were stained with crystal violet. We determined that a higher number of gremlin-1-A549 cells migrated as compared to mock-A549 cells (Fig. 14C, ***$P<0.001$). In a scratch wound healing assay, gremlin-1-A549 cells also showed increased migration as compared with mock-A549 cells, and migration was significantly inhibited upon addition of the neutralizing antibody GRE1 (Fig. 14D, **$P<0.01$, ***$P<0.001$). To

identify whether gremlin-1 influences cell growth, a cell proliferation assay was performed. Gremlin-1-A549 cells had a higher growth rate compared to mock-A549 cells or untransfected A549 cells (Fig. 14E, *P<0.05). The increased growth rate of gremlin-1-A549 cells was inhibited by the addition of the neutralizing antibody GRE1 (Fig. 14E).

Gremlin-1 enhances tumor growth in vivo

To evaluate the effect of gremlin-1 on tumorigenesis, gremlin-1-A549 cells or mock-A549 cells were injected subcutaneously into nude mice. Tumor size was measured weekly using a digital caliper. The tumor volume in mice injected with gremlin-1-A549 cells increased more rapidly than those injected with mock-A549 cells, with an approximately 500 mm^3 difference in tumor volume at 14 weeks post injection (Fig. 14F). This result suggests that increased expression of gremlin-1 may play a role in tumorigenesis.

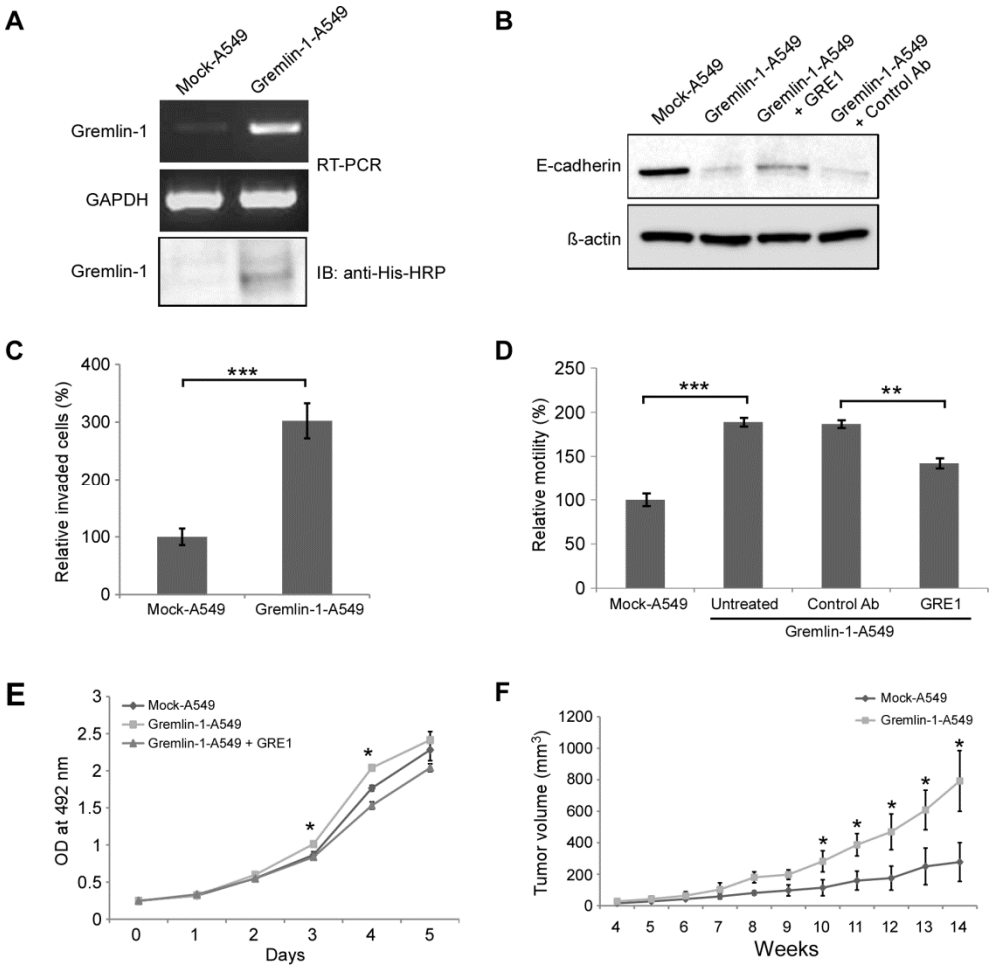

Figure 14. Characterization of gremlin-1-transfected A549 cell lines.

(A) RT-PCR and western blot analyses indicate gremlin-1 mRNA and protein are expressed in gremlin-1-A549 cells but not mock-A549 cells. (B) E-cadherin protein expression is reduced in gremlin-1-A549 cells and this effect is attenuated upon addition of the neutralizing antibody GRE1. (C) Gremlin-1-A549 cells show

increased invasiveness in cell invasion assays as compared to mock-A549 cells. The cells on the underside of the ECM membrane were stained and counted. ***P<0.001, Student's *t* test. (D) Gremlin-1-A549 cells show increased migration compared to mock-A549 cells and this effect is attenuated upon the addition of the neutralizing antibody GRE1. **P<0.01, ***P<0.001, Student's *t* test. (E) Gremlin-1-A549 cells display an increased growth rate compared to mock-A549 cells as determined by MTS proliferation assay. The neutralizing antibody GRE1 addition blocks this effect. *P<0.05 versus mock-A549, Student's *t* test. (F) Gremlin-1-A549 cells injected subcutaneously in nude mice have an increased rate of tumor growth *in vivo* as compared with injection of mock-A549 cells. Tumor volume is depicted as the average ± standard deviation. *P<0.05 versus mock-A549, Student's *t* test.

Discussion

Gremlin-1 has a critical role regulating BMPs during embryonic development but its expression is down-regulated in normal adult tissues (8, 9). Differential display RT-PCR analysis revealed that gremlin-1 is overexpressed in various human tumors including carcinoma of the lung, ovary, kidney, breast, colon, pancreas, and cervix (25). It was also reported that gremlin-1 is overexpressed in the stroma of basal cell carcinoma (BCC) but not in normal skin according to immunohistochemical analysis. In *in situ* hybridization analyses, elevated gremlin-1 mRNA levels were detected in various cancer tissues, including esophagus, bladder, and prostate (26). However, the function of gremlin-1 in carcinogenesis has not yet been elucidated.

In this study, we report that gremlin-1 interacts with various cancer cell lines (Fig. 10). Recently it was reported that gremlin-1 interacts with VEGFR2 and induces angiogenic responses *in vitro* and *in vivo* (23). We evaluated whether VEGFR2 was responsible for the interaction of gremlin-1 with cancer cells. We did not detect VEGFR2 expression in A549 or HeLa cells though both cell lines strongly interacted with gremlin-1 (Fig. 11). Therefore, we

conclude that gremlin-1 can bind cancer cells and this binding is not mediated by VEGFR2.

Gremlin-1 is a BMP antagonist that specifically binds to and inhibits the activity of BMP-2, BMP-4, and BMP-7 (5, 6). BMPs are multi-functional growth factors known to play important roles in morphogenesis and homeostasis of many tissues. In addition, BMP-2, BMP-4, and BMP-7 are frequently overexpressed in various cancers including breast and prostate (36-38). It was reported that BMP-4 reduced the proliferation of BCC cells and addition of gremlin-1 reduced the anti-proliferative effect of BMP-4 indirectly (26). We verified that the mRNA levels of BMP-2 and BMP-4 were highly expressed in A549 cells (data not shown). We also evaluated the interaction of gremlin-1 with A549 cells in the presence of BMP-2, BMP-4, or BMP-7. We determined that gremlin-1 strongly bound BMP-2 and BMP-4 (Fig. 12A) but this binding did not affect its interaction with cancer cells (Fig. 12B). In addition, the neutralizing antibody GRE1 did not inhibit the binding of gremlin-1 to BMP-2 or BMP-4 (Fig. 12A). Therefore, we conclude the interaction of gremlin-1 with A549 cells is likely mediated by a different motif than the motif involved in the interaction with BMPs.

When A549 cells were incubated with gremlin-1, the cell morphology became fibroblast-like and cells were scattered (Fig. 13A). We also found decreased E-cadherin expression when cells were incubated with gremlin-1 (Fig. 13B, 13C, and 14B). E-cadherin is a major epithelial cell-to-cell adhesion molecule that functions as a tumor suppressor. E-cadherin deficiency plays a causative role in tumor cell invasion and metastasis (39-41). Down-regulation of E-cadherin is associated with epithelial-mescenchymal transition (EMT) and EMT plays a main part in cancer progression, particularly during invasion and intravasation process when tumor cells migrate to distant organs to form metastases (42, 43). One of the earliest steps in EMT is the suppression of the epithelial marker, E-cadherin (44). In a scratch wound healing assay, gremlin-1 increased the migration of A549 cells. Addition of the neutralizing antibody GRE1 suppressed the observed increase in migration (Fig. 13D and 14D). Furthermore, gremlin-1-A549 cells showed increased invasion through the ECM-coated membrane. It was previously reported that transfection of A549 cells with gremlin-1 sensitized the cells to EMT upon treatment with TGF-β1 (45). However, induction of an EMT-like phenotype by gremlin-1 alone has not been reported.

Gremlin-1-A549 cells also showed increased proliferation *in vitro* and *in vivo* (Fig. 14E & 14F). In an *In vitro* setting, the increased proliferation rate was reduced upon addition of the GRE1 antibody. Experiments are currently underway to investigate if gremlin-1 directly influences tumor growth. These data suggest that the secretion of gremlin-1 may increase cell proliferation and thus affect tumorigenesis.

Further experiments are required to determine the receptor which has reactivity with gremlin-1 and to understand a receptor-mediated mechanism of action in cancer. Also, anti-gremlin-1 antibodies which recognize various epitopes of gremlin-1 with high affinity should be developed for use as diagnostic and therapeutic agents.

REFERENCES

1. Topol LZ, Marx M, Laugier D, Bogdanova NN, Boubnov NV, Clausen PA, et al. Identification of drm, a novel gene whose expression is suppressed in transformed cells and which can inhibit growth of normal but not transformed cells in culture. Molecular and cellular biology. 1997;17(8):4801-10. Epub 1997/08/01.

2. Topol LZ, Modi WS, Koochekpour S, Blair DG. DRM/GREMLIN (CKTSF1B1) maps to human chromosome 15 and is highly expressed in adult and fetal brain. Cytogenetics and cell genetics. 2000;89(1-2):79-84. Epub 2000/07/15.

3. Wordinger RJ, Zode G, Clark AF. Focus on molecules: gremlin. Experimental eye research. 2008;87(2):78-9. Epub 2008/01/19.

4. Topol LZ, Bardot B, Zhang Q, Resau J, Huillard E, Marx M, et al. Biosynthesis, post-translation modification, and functional characterization of Drm/Gremlin. The Journal of biological

chemistry. 2000;275(12):8785-93. Epub 2000/03/18.

5. Stanley E, Biben C, Kotecha S, Fabri L, Tajbakhsh S, Wang CC, et al. DAN is a secreted glycoprotein related to Xenopus cerberus. Mechanisms of development. 1998;77(2):173-84. Epub 1998/11/30.

6. Merino R, Rodriguez-Leon J, Macias D, Ganan Y, Economides AN, Hurle JM. The BMP antagonist Gremlin regulates outgrowth, chondrogenesis and programmed cell death in the developing limb. Development. 1999;126(23):5515-22. Epub 1999/11/11.

7. Lappin DW, Hensey C, McMahon R, Godson C, Brady HR. Gremlins, glomeruli and diabetic nephropathy. Current opinion in nephrology and hypertension. 2000;9(5):469-72. Epub 2000/09/16.

8. Lu MM, Yang H, Zhang L, Shu W, Blair DG, Morrisey EE. The bone morphogenic protein antagonist gremlin regulates proximal-distal patterning of the lung. Developmental dynamics : an official publication of the American Association of Anatomists.

2001;222(4):667-80. Epub 2001/12/19.

9. Shi W, Zhao J, Anderson KD, Warburton D. Gremlin negatively modulates BMP-4 induction of embryonic mouse lung branching morphogenesis. American journal of physiology Lung cellular and molecular physiology. 2001;280(5):L1030-9. Epub 2001/04/06.

10. Michos O, Panman L, Vintersten K, Beier K, Zeller R, Zuniga A. Gremlin-mediated BMP antagonism induces the epithelial-mesenchymal feedback signaling controlling metanephric kidney and limb organogenesis. Development. 2004;131(14):3401-10. Epub 2004/06/18.

11. Costello CM, Cahill E, Martin F, Gaine S, McLoughlin P. Role of gremlin in the lung: development and disease. American journal of respiratory cell and molecular biology. 2010;42(5):517-23. Epub 2009/07/04.

12. Khokha MK, Hsu D, Brunet LJ, Dionne MS, Harland RM. Gremlin is the BMP antagonist required for maintenance of Shh and

Fgf signals during limb patterning. Nature genetics. 2003;34(3):303-7. Epub 2003/06/17.

13. Gazzerro E, Pereira RC, Jorgetti V, Olson S, Economides AN, Canalis E. Skeletal overexpression of gremlin impairs bone formation and causes osteopenia. Endocrinology. 2005;146(2):655-65. Epub 2004/11/13.

14. Gazzerro E, Smerdel-Ramoya A, Zanotti S, Stadmeyer L, Durant D, Economides AN, et al. Conditional deletion of gremlin causes a transient increase in bone formation and bone mass. The Journal of biological chemistry. 2007;282(43):31549-57. Epub 2007/09/06.

15. Dolan V, Murphy M, Alarcon P, Brady HR, Hensey C. Gremlin - a putative pathogenic player in progressive renal disease. Expert opinion on therapeutic targets. 2003;7(4):523-6. Epub 2003/07/30.

16. Zuniga A, Haramis AP, McMahon AP, Zeller R. Signal relay by BMP antagonism controls the SHH/FGF4 feedback loop in

vertebrate limb buds. Nature. 1999;401(6753):598-602. Epub 1999/10/19.

17. Mass RL, Zeller R, Woychik RP, Vogt TF, Leder P. Disruption of formin-encoding transcripts in two mutant limb deformity alleles. Nature. 1990;346(6287):853-5. Epub 1990/08/30.

18. McMahon R, Murphy M, Clarkson M, Taal M, Mackenzie HS, Godson C, et al. IHG-2, a mesangial cell gene induced by high glucose, is human gremlin. Regulation by extracellular glucose concentration, cyclic mechanical strain, and transforming growth factor-beta1. The Journal of biological chemistry. 2000;275(14):9901-4. Epub 2000/04/01.

19. Dolan V, Murphy M, Sadlier D, Lappin D, Doran P, Godson C, et al. Expression of gremlin, a bone morphogenetic protein antagonist, in human diabetic nephropathy. American journal of kidney diseases : the official journal of the National Kidney Foundation. 2005;45(6):1034-9. Epub 2005/06/16.

20. Boers W, Aarrass S, Linthorst C, Pinzani M, Elferink RO, Bosma P. Transcriptional profiling reveals novel markers of liver fibrogenesis: gremlin and insulin-like growth factor-binding proteins. The Journal of biological chemistry. 2006;281(24):16289-95. Epub 2006/04/12.

21. Sun J, Zhuang FF, Mullersman JE, Chen H, Robertson EJ, Warburton D, et al. BMP4 activation and secretion are negatively regulated by an intracellular gremlin-BMP4 interaction. The Journal of biological chemistry. 2006;281(39):29349-56. Epub 2006/08/02.

22. Chen B, Blair DG, Plisov S, Vasiliev G, Perantoni AO, Chen Q, et al. Cutting edge: bone morphogenetic protein antagonists Drm/Gremlin and Dan interact with Slits and act as negative regulators of monocyte chemotaxis. J Immunol. 2004;173(10):5914-7. Epub 2004/11/06.

23. Mitola S, Ravelli C, Moroni E, Salvi V, Leali D, Ballmer-Hofer K, et al. Gremlin is a novel agonist of the major proangiogenic receptor VEGFR2. Blood. 2010;116(18):3677-80. Epub 2010/07/28.

24. Sha G, Zhang Y, Zhang C, Wan Y, Zhao Z, Li C, et al. Elevated levels of gremlin-1 in eutopic endometrium and peripheral serum in patients with endometriosis. Fertility and sterility. 2009;91(2):350-8. Epub 2008/03/04.

25. Namkoong H, Shin SM, Kim HK, Ha SA, Cho GW, Hur SY, et al. The bone morphogenetic protein antagonist gremlin 1 is overexpressed in human cancers and interacts with YWHAH protein. BMC cancer. 2006;6:74. Epub 2006/03/21.

26. Sneddon JB, Zhen HH, Montgomery K, van de Rijn M, Tward AD, West R, et al. Bone morphogenetic protein antagonist gremlin 1 is widely expressed by cancer-associated stromal cells and can promote tumor cell proliferation. Proceedings of the National Academy of Sciences of the United States of America. 2006;103(40):14842-7. Epub 2006/09/28.

27. Hoogenboom HR. Overview of antibody phage-display technology and its applications. Methods Mol Biol. 2002;178:1-37. Epub 2002/04/24.

28. Winter G, Griffiths AD, Hawkins RE, Hoogenboom HR. Making antibodies by phage display technology. Annual review of immunology. 1994;12:433-55. Epub 1994/01/01.

29. Hoogenboom HR, Chames P. Natural and designer binding sites made by phage display technology. Immunology today. 2000;21(8):371-8. Epub 2000/08/01.

30. Park S, Lee DH, Park JG, Lee YT, Chung J. A sensitive enzyme immunoassay for measuring cotinine in passive smokers. Clinica chimica acta; international journal of clinical chemistry. 2010;411(17-18):1238-42. Epub 2010/05/05.

31. Lee MS, Lee JC, Choi CY, Chung J. Production and characterization of monoclonal antibody to botulinum neurotoxin type B light chain by phage display. Hybridoma (Larchmt). 2008;27(1):18-24. Epub 2008/02/26.

32. Chung J, Rader C, Popkov M, Hur YM, Kim HK, Lee YJ, et al. Integrin alphaIIbbeta3-specific synthetic human monoclonal

antibodies and HCDR3 peptides that potently inhibit platelet aggregation. The FASEB journal : official publication of the Federation of American Societies for Experimental Biology. 2004;18(2):361-3. Epub 2003/12/23.

33. Li XL, Wang CZ, Mehendale SR, Sun S, Wang Q, Yuan CS. Panaxadiol, a purified ginseng component, enhances the anti-cancer effects of 5-fluorouracil in human colorectal cancer cells. Cancer chemotherapy and pharmacology. 2009;64(6):1097-104. Epub 2009/03/12.

34. Rosso O, Piazza T, Bongarzone I, Rossello A, Mezzanzanica D, Canevari S, et al. The ALCAM shedding by the metalloprotease ADAM17/TACE is involved in motility of ovarian carcinoma cells. Molecular cancer research : MCR. 2007;5(12):1246-53. Epub 2008/01/04.

35. Tomayko MM, Reynolds CP. Determination of subcutaneous tumor size in athymic (nude) mice. Cancer chemotherapy and pharmacology. 1989;24(3):148-54. Epub 1989/01/01.

36. Singh A, Morris RJ. The Yin and Yang of bone morphogenetic proteins in cancer. Cytokine & growth factor reviews. 2010;21(4):299-313. Epub 2010/08/07.

37. Chen D, Zhao M, Mundy GR. Bone morphogenetic proteins. Growth Factors. 2004;22(4):233-41. Epub 2004/12/29.

38. Bobinac D, Maric I, Zoricic S, Spanjol J, Dordevic G, Mustac E, et al. Expression of bone morphogenetic proteins in human metastatic prostate and breast cancer. Croatian medical journal. 2005;46(3):389-96. Epub 2005/04/30.

39. Vleminckx K, Vakaet L, Jr., Mareel M, Fiers W, van Roy F. Genetic manipulation of E-cadherin expression by epithelial tumor cells reveals an invasion suppressor role. Cell. 1991;66(1):107-19. Epub 1991/07/12.

40. Frixen UH, Behrens J, Sachs M, Eberle G, Voss B, Warda A, et al. E-cadherin-mediated cell-cell adhesion prevents invasiveness of human carcinoma cells. The Journal of cell biology. 1991;113(1):173-85. Epub 1991/04/01.

41. Perl AK, Wilgenbus P, Dahl U, Semb H, Christofori G. A causal role for E-cadherin in the transition from adenoma to carcinoma. Nature. 1998;392(6672):190-3. Epub 1998/03/27.

42. Thiery JP. Epithelial-mesenchymal transitions in tumour progression. Nature reviews Cancer. 2002;2(6):442-54. Epub 2002/08/22.

43. Gupta GP, Massague J. Cancer metastasis: building a framework. Cell. 2006;127(4):679-95. Epub 2006/11/18.

44. Yang J, Liu Y. Dissection of key events in tubular epithelial to myofibroblast transition and its implications in renal interstitial fibrosis. The American journal of pathology. 2001;159(4):1465-75. Epub 2001/10/05.

45. Koli K, Myllarniemi M, Vuorinen K, Salmenkivi K, Ryynanen MJ, Kinnula VL, et al. Bone morphogenetic protein-4 inhibitor gremlin is overexpressed in idiopathic pulmonary fibrosis. The American journal of pathology. 2006;169(1):61-71. Epub

2006/07/04.

ABSTRACT IN KOREAN

골형성 촉진 단백질(BMP) 억제 물질 중 하나인 그렘린-1은 다양한 암 관련 조직에서 과발현되어 있지만 발암과정에서 이 단백질의 역할은 아직 규명되지 않았다. 본 연구에서 그렘린-1과 결합력을 보이는 여러 종류의 암 세포주를 선별하였고, 새롭게 제작한 항-그렘린-1 항체를 처리하여 그렘린-1과 암세포주의 결합력이 저해되는 것을 확인하였다. 골형성 촉진 단백질-2, -4, 및 -7이 존재하는 조건에서 암 세포주와 그렘린-1의 결합력은 영향을 받지 않는 것을 확인하였다. 그렘린-1의 암세포 결합은 세포 표면에 발현되어 있는 혈관 내피세포 성장인자 수용체-2(VEGFR-2)와 무관하였다. 폐암 세포주 A549에 그렘린-1을 처리하면, 세포 모양이 섬유아세포성 형태(fibroblast-like morphology)로 변하였고, 이케드헤린(E-cadherin)의 발현양이 감소하였다. 상처치유 분석(a scratch wound healing assay)을 통해서, 그렘린-1을 처리한 세포나 그렘린-1을 형질주입한 세포에서 세포 이동성이 향상되는 효과를 보였고, 항-그렘린-1 항체를 처리하면 세포 이동성이 다시 감소하는 것을 확인하였다. 그렘린-1을 형질주입한 세포는 세포 성장률과 침윤성이 증가하였고, 이는 항-그렘린-1 항체에 의해 저해되었다. 요약하면, 본 연구는 골형성 촉진 단백질과 혈관 내피세포 성장인자 수용체-2와는 무관하게 그렘린-1이 다양한 암 세포주와 결합하고, 암세포주의 세포 증식, 이동 및 침윤을 유도함을 입증하였다.

주요어: 그렘린-1, 암세포주, 폐암 세포주 A549, 세포 증식, 이동, 침윤, 파지 디스플레이, 단일항체

학번: 2006-22170